

Pentacyclic Triterpenoids from *Astilbe rivularis* that Enhance Glucose Uptake via the Activation of Akt and Erk1/2 in C2C12 Myotubes

Joo-Hui Han,^{†,▽} Wei Zhou,^{‡,§,▽} Wei Li,[⊥] Pham Quoc Tuan,^{||} Nguyen Minh Khoi,^{||}
Phuong Thien Thuong,^{||} MinKyun Na,^{*,‡,#} and Chang-Seon Myung^{*,†,‡,#}

[†]Departments of Pharmacology, and [‡]Pharmacognosy, Chungnam National University College of Pharmacy, Daejeon 305-764, Republic of Korea

[§]College of Pharmacy, Yanbian University, Yanji 133002, People's Republic of China

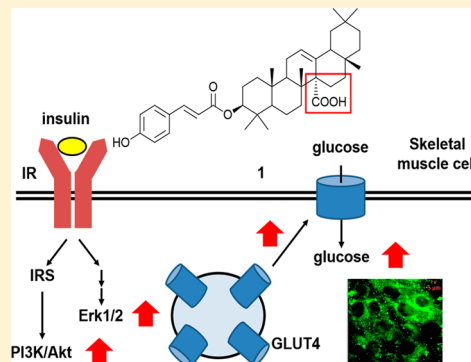
[⊥]School of Biotechnology, Yeungnam University, Gyeongsan, Gyeongbuk 712-749, Republic of Korea

^{||}National Institute of Medicinal Materials, 3B Quang Trung, Hoan Kiem, Hanoi, Vietnam

^{*}Institute of Drug Research & Development, Chungnam National University, Daejeon 305-764, Republic of Korea

Supporting Information

ABSTRACT: Glucose uptake into insulin-sensitive tissues is important for the regulation of blood glucose. This study has investigated whether the pentacyclic triterpenoids substituted with a carboxylic acid at the C-27 position isolated from *Astilbe rivularis* can enhance glucose uptake and subsequently to also examine their underlying molecular mechanisms. The structure of the new pentacyclic triterpenoid **1** was assigned by spectroscopic data interpretation. To evaluate the activity of compounds **1** and **2**, glucose uptake and glucose transporter 4 (GLUT4) translocation were measured in C2C12 myotubes. The C-27-carboxylated triterpenoids **1** and **2** significantly increased basal and insulin-stimulated glucose uptake and GLUT4 translocation to plasma membrane. Both compounds stimulated the phosphorylation of insulin receptor substrate-1 (IRS-1), protein kinase B (Akt), and extracellular signal-regulated kinase 1/2 (Erk1/2). Pretreatment with the Akt inhibitor triciribine or the Erk1/2 inhibitor U0126 decreased the ability of both compounds to enhance basal- and insulin-stimulated glucose uptake and stimulate GLUT4 translocation. These results indicate that compounds **1** and **2** activated both the IRS-1/Akt and Erk1/2 pathways and subsequently stimulated GLUT4 translocation, leading to enhanced glucose uptake. Thus, these observations suggest that C-27-carboxylated-pentacyclic triterpenoids may serve as scaffolds for development as agents for the management of blood glucose levels in disease states such as diabetes.



Diabetes mellitus is characterized by the failure to maintain blood glucose levels. Among diabetes patients, type 2 diabetes accounts for about 90% of all diabetes cases.¹ Insulin resistance, characterized by decreased insulin sensitivity, is a key feature of type 2 diabetes and is caused by impaired glucose uptake into skeletal muscle and adipose tissue.² Postprandial glucose uptake induced by insulin occurs predominantly into skeletal muscle because the skeletal muscle accounts for nearly 40% of the body mass of humans and 80% of glucose absorption during insulin stimulation.³

Glucose uptake is achieved by glucose transporters, which are membrane proteins that facilitate the transport of glucose across the plasma membrane.⁴ Among 13 transporter proteins in the human body, glucose transporter 4 (GLUT4) is highly expressed in skeletal muscle and is actually translocated to the plasma membrane by insulin and other stimuli, as, for example, by exercise and muscle contraction.⁵

There are two major signaling pathways for the stimulation of glucose uptake in skeletal muscle. One is an insulin-dependent pathway, which involves insulin receptor substrate (IRS)-, phosphatidylinositol 3-kinase (PI3K)-, and protein kinase B

(Akt)-mediated signaling activated by the interaction of insulin with its receptor. IRS mediates diverse metabolic and mitogenic responses of insulin.⁶ Among the six IRS proteins identified, IRS-1 and IRS-2 are major substrates in the regulation of glucose metabolism.⁷ It is known that, on insulin-mediated signal transduction, IRS-1 is more important for Akt activation than IRS-2; however, IRS-2 is more important in extracellular signal-regulated kinases 1/2 (Erk1/2) activation.⁸ Erk1/2, a mitogen-activated protein kinase (MAPK) family component, is related to cell proliferation, growth, and survival. However, activation of the PI3K/Erk1/2 pathway by acute palmitate treatment stimulates glucose uptake in skeletal muscle cells.⁹ Furthermore, Erk1/2 activation can phosphorylate Akt substrates of 160 kDa (AS160), as a key protein in controlling GLUT4 trafficking, via p90 ribosomal protein S6 kinase (p90RSK) in 3T3-L1 adipocytes.¹⁰

The other signaling pathway is the insulin-independent pathway, which is mediated by 5'-adenosine monophosphate-activated

Received: November 18, 2014

Published: April 20, 2015

protein kinase (AMPK) and p38 MAPK. p38 MAPK is a main effector kinase for AMPK and can be activated by exercise and muscle contraction.^{11,12} The activation of p38 MAPK in resting muscle by the p38 activator anisomycin stimulates glucose uptake,¹³ implying enhanced insulin sensitivity. However, this finding is controversial. Another study reported that the p38 MAPK inhibitor SB203580 blocks insulin-stimulated glucose uptake, not by suppressing p38 MAPK phosphorylation but by directly binding to GLUT4 and decreasing GLUT4 transport activity in the soleus muscle.¹⁴ Thus, p38 MAPK may not be the main signaling molecule for insulin-stimulated glucose uptake.

Protein tyrosine phosphatase-1B (PTP-1B) is a negative regulator of the insulin-signaling pathway by dephosphorylating the phosphotyrosine residues of the activated insulin receptor kinase.¹⁵ PTP-1B is widely expressed in insulin-sensitive tissues, and its overexpression results in an insulin-resistant state.¹⁶ It is reported that PTP-1B knockdown improves insulin sensitivity in palmitate-induced insulin resistance skeletal muscle cells.¹⁷ Several PTP-1B inhibitors can enhance glucose uptake in adipocytes and myotubes.^{18,19} Thus, blocking of PTP-1B can stimulate glucose uptake, leading to improved insulin sensitivity.

It was reported recently that pentacyclic triterpenoids increased glucose uptake, possibly through inhibition of PTP-1B.^{20–22} Plant-derived triterpenoids, particularly those with ursane- and cucurbitane-type carbon skeleton, have been reported to exert antidiabetic effects through various mechanisms in various cell types. Corosolic acid and ursolic acid, which are ursane-type triterpenoids with a carboxylic acid group at C-28, were shown to enhance insulin receptor phosphorylation in CHO/hIR cells and stimulate glucose uptake in L6 myotubes.^{21,22} Cucurbitane triterpenoids from bitter melon stimulated GLUT4 translocation both in L6 myotubes and 3T3-L1 adipocytes, and these activities were associated with activation of the AMP-activated protein kinase (AMPK) pathway.²³ Triterpenoids isolated from the bark of *Paeonia suffruticosa* were demonstrated to increase glucose uptake and glycogen synthesis via AMPK activation in insulin-resistant human HepG2 cells.²⁴ These results provided the motivation to explore new pentacyclic triterpenes capable of inhibiting the target enzyme. The genus *Astilbe* is recognized as a source of characteristic pentacyclic triterpenoids substituted with a carboxylic acid group at the C-27 position.²⁰ Plant-derived triterpenoids have been demonstrated to inhibit PTP-1B,²⁰ which provided a rationale to investigate various pentacyclic triterpenoids having a carboxylic acid at C-27 from *A. rivularis*. Most plant-derived pentacyclic triterpenoids have a carboxylic acid at the C-28 position, while C-27 carboxylated-pentacyclic triterpenoids have been detected mainly in the plant families of Saxifragaceae, Boraginaceae, Meliaceae, and Lamiaceae.^{25–27}

The plant *Astilbe rivularis* Buch.-Ham. (Saxifragaceae) is a perennial herb that grows in mountains and moist shrubbery and is distributed mainly in Nepal, Vietnam, the northern parts of India, and southwestern mainland China. The current chemical investigation on the roots of *A. rivularis* resulted in the isolation of a new pentacyclic triterpene, 3 β -trans-p-coumaroyloxy-olean-12-en-27-oic acid (**1**), along with five known triterpenoids, of which 6 β -hydroxy-3-oxoolean-12-en-27-oic acid (**2**)²⁸ was obtained from the genus *Astilbe* for the first time. The structure of the new compound **1** is related to that of aceriphylllic acid G, 3 α -O-caffeoylean-12-en-27-oic acid, isolated from *Aceriphyllum rossii* (Saxifragaceae).²⁹ With the exception of a previous report that pentacyclic triterpenes with a C-27 carboxylic acid group inhibit PTP-1B activity,²⁰ no mechanism-based study concerning the potential antidiabetic effect of this type of triterpenoids

has been published to date. The present study has investigated the effect of pentacyclic triterpenoids with a C-27 carboxylic acid unit on glucose uptake in C2C12 myotubes and in clarifying the underlying molecular mechanism, focusing on insulin-dependent and -independent pathways.

RESULTS AND DISCUSSION

Compound **1** was obtained as a white amorphous powder, and the molecular formula was established as C₃₉H₅₄O₅ by HRESIMS data at *m/z* 625.3870 [M + Na]⁺ (calcd for C₃₉H₅₄O₅Na, 625.3869). The ¹H NMR spectrum of **1** (Table 1) showed

Table 1. NMR Spectroscopic Data (600 MHz, Pyridine-*d*₅) for Compound **1**

position	δ_{C} , type	δ_{H} , mult (<i>J</i> in Hz)
1	37.7, CH ₂	1.48, m
2	23.7, CH ₂	1.89, 1.72, m
3	78.2, CH	5.02, t (2.4)
4	37.5, C	
5	51.1, CH	1.62, d (12.0)
6	18.9, CH ₂	1.48, 1.33, m
7	37.4, CH ₂	1.89, 1.79, m
8	40.3, C	
9	47.8, CH	2.91, dd (11.5, 5.2)
10	34.7, C	
11	23.6, CH ₂	1.96, 1.89, m
12	125.8, CH	5.80, t (3.4)
13	139.0, C	
14	57.0, C	
15	23.4, CH ₂	2.42, d (13.4), 2.11, m
16	28.8, CH ₂	2.48, td (13.4, 3.6), 2.01, m
17	33.7, C	
18	50.3, CH	2.21, dd (13.5, 3.6)
19	44.8, CH ₂	1.79, 1.33, m
20	31.6, C	
21	35.1, CH ₂	1.07, m
22	37.3, CH ₂	1.26, m
23	28.4, CH ₃	0.91, s
24	22.4, CH ₃	0.89, s
25	16.7, CH ₃	1.00, s
26	18.9, CH ₃	1.14, s
27	178.7, C	
28	29.0, CH ₃	1.03, s
29	24.2, CH ₃	0.89, s
30	33.8, CH ₃	0.74, s
1'	167.2, C	
2'	116.3, CH	6.58, d (15.8)
3'	145.2, CH	8.00, d (15.8)
4'	126.5, C	
5'	131.0, CH	7.53, d (8.6)
6'	117.1, CH	7.04, d (8.6)
7'	161.7, C	
8'	117.1, CH	7.04, d (8.6)
9'	131.0, CH	7.53, d (8.6)

signals of an olefinic proton at δ_{H} 5.80 (1H, t, *J* = 3.4 Hz), an oxygenated methine proton at δ_{H} 5.02 (1H, t, *J* = 2.4 Hz), and seven tertiary methyls at δ_{H} 0.74, 0.89 ($\times 2$), 0.91, 1.00, 1.03, 1.14 (each 3H, s). In addition, a 1,4-disubstituted aromatic ring at δ_{H} 7.53 (2H, d, *J* = 8.6 Hz) and 7.04 (2H, d, *J* = 8.6 Hz) and two olefinic protons at δ_{H} 8.00 (1H, d, *J* = 15.8 Hz) and 6.58 (1H, d, *J* = 15.8 Hz) suggested the presence of a *trans*-p-coumaroyl

moiety in **1**. The ^{13}C NMR spectrum (Table 1) revealed 39 carbon signals, comprising seven methyls, 10 methylenes, 11 methines, and 11 quaternary carbons. The presence of a double bond at δ_{C} 139.0 and 125.8, a hydroxymethine at δ_{C} 78.2, and seven tertiary methyls at δ_{C} 33.8, 29.0, 28.4, 24.2, 22.4, 18.9, and 16.7 indicated that the framework of **1** is an oleanane-type triterpene, and its NMR spectroscopic data were found to be similar to those of 3β -hydroxyolean-12-en-27-oic acid.³⁰ Thus, **1** could be assigned as a 3β -hydroxyolean-12-en-27-oic acid derivative containing a *trans*-*p*-coumaroyl group. All of the ^1H and ^{13}C NMR signals of **1** were assigned based on HMQC, HMBC, COSY, and NOESY spectroscopic data analysis (Figures S4–S7, Supporting Information). In the HMBC spectrum, the oxygenated methine proton signal at H-3 (δ_{H} 5.02) correlated with C-1 (δ_{C} 37.7), C-5 (δ_{C} 51.1), C-24 (δ_{C} 22.4), and C-1' (δ_{C} 167.2), suggesting that the *trans*-*p*-coumaroyl moiety should be located at C-3. The HMBC correlation between H-15 (δ_{H} 2.42, 2.11) and C-27 (δ_{C} 178.7) revealed the location of carboxylic acid group at C-27 (Figure 1A). The orientation of H-3 was

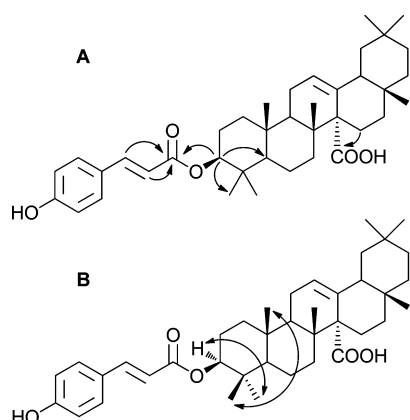


Figure 1. Key HMBC (→) and NOESY (↔) correlations of compound **1**.

established as α -equatorial from the NOESY correlation between H-3 (δ_{H} 5.02) and H-23 (δ_{H} 0.91) (Figure 1B). On the basis of the above analysis, the structure of **1** was proposed as 3β -*trans*-*p*-coumaroyloxy-olean-12-en-27-oic acid.

Compound **2** was identified as 6β -hydroxy-3-oxoolean-12-en-27-oic acid, which was isolated recently from *Chrysosplenium carnosum* (Saxifragaceae).²⁸ However, this is the first report of the compound from the genus *Astilbe*. The other triterpenes isolated in this study were identified as 3β -hydroxyolean-12-en-27-oic acid,²⁸ $3\beta,6\beta$ -dihydroxyolean-12-en-27-oic acid,²⁸ $3\beta,24$ -dihydroxyolean-12-en-27-oic acid,³¹ and $3\beta,6\beta,7\alpha$ -trihydroxy-olean-12-en-27-oic acid,³² based on analysis of their spectroscopic data and comparison with literature values.

In the process of an activity-finding screening assay using *p*-nitrophenyl phosphate as the substrate in vitro, compounds **1** and **2** strongly inhibited over 90% of the enzyme activity of PTP-1B at 30 μM (data not shown). To determine the effect of compounds on glucose uptake in vitro, mouse skeletal muscle cell line C2C12 myotubes were treated with **2** at the indicated time points. As shown in Figure 2A, 40 μM **2** enhanced basal or insulin-stimulated glucose uptake from 15 min and was maximally increased at 2 h and then decreased gradually. Thus, in this study, the 2 h time point was used for treatment with the compounds. Figure 2B illustrates that, as the concentrations of compounds increased, basal or insulin stimulated-glucose uptake was enhanced. When the highest concentration of **1** and **2**

(40 μM) was used for treatment, basal glucose uptake was increased significantly by $19.1 \pm 4.3\%$ and $23.9 \pm 8.5\%$, respectively, and insulin-stimulated glucose uptake was increased significantly by $44.6 \pm 4.6\%$ and $62.8 \pm 12.7\%$, respectively. To compare this effect, 30 μM rosiglitazone (thiazolidinedione class)³³ and 10 μM ursolic acid (PTP-1B inhibitor)³⁴ were used as positive controls. These inhibitors also significantly increased the basal glucose uptake by $18.3 \pm 6.1\%$ and $19.4 \pm 7.1\%$, respectively, and insulin-stimulated glucose uptake by $46.9 \pm 4.4\%$ and $47.7 \pm 3.8\%$, respectively. To determine the cytotoxicity of **1**–**6**, the MTT assay was performed. Figure 2C shows that **1** and **2** (20 and 40 μM) did not exert cytotoxicity in C2C12 myotubes upon incubation in cells for 2 or 4 h. However, 3β -hydroxyolean-12-en-27-oic acid, $3\beta,24$ -dihydroxyolean-12-en-27-oic acid, and $3\beta,6\beta,7\alpha$ -trihydroxyolean-12-en-27-oic acid showed cytotoxicity (Figure S15, Supporting Information). $3\beta,6\beta$ -Dihydroxyolean-12-en-27-oic acid exerted no marked effect on glucose uptake (data not shown). Thus, subsequent experiments were carried out using **1** and **2**. Neither rosiglitazone (30 μM) nor ursolic acid (10 μM) showed cytotoxicity in C2C12 myotubes. Digitonin (100 $\mu\text{g}/\text{mL}$), a well-known membrane-permeabilizing reagent, was used as a positive control.³⁵

In insulin-sensitive cells, such as skeletal muscle cells and adipocytes, stimulation of glucose uptake is mediated mainly by a specific transporter, GLUT4, which is translocated from GLUT4 vesicles in the cytoplasm to the plasma membrane.³⁶ To determine whether the ability of compounds to enhance glucose uptake is correlated with increased GLUT4 translocation, immunofluorescence was performed. Figure 3A shows optical images and demonstrates that compounds increase GLUT4 translocation under both basal- and insulin-stimulated conditions. The positive controls, rosiglitazone (30 μM) and ursolic acid (10 μM), also enhanced GLUT4 translocation. The relative density of GLUT4 translocation is presented in Figure 3B.

Insulin signaling is regulated by various signaling networks. The first is activation of the insulin receptor (IR) tyrosine kinase, leading to IRS tyrosine phosphorylation. Among the negative regulators of this stage, PTP-1B acts directly on IR and dephosphorylates IRS tyrosine residues, finally reducing insulin sensitivity.³⁷ Although IRS-1 and IRS-2 are widely distributed, and degradation of both subtypes causes insulin resistance, IRS-1 and IRS-2 are thought to have tissue-specific effects and participate differently in signal molecule activation. According to previous knockout studies in vivo,³⁸ either IRS-1 or IRS-2 acts on muscle, but IRS-2 acts mainly on liver and adipose tissue. Moreover, IRS-1 primarily regulates the phosphorylation of Akt, mainly at Ser⁴⁷³ and partly at Thr³⁰⁸, and regulates AS160. However, IRS-2 phosphorylates Akt at Thr³⁰⁸ and Erk1/2, and partially phosphorylates AS160.⁸ Phosphorylation of AS160 by upstream proteins results in GLUT4 storage vesicle (GSV) fusion with the plasma membrane, resulting in increased glucose uptake.

To investigate the role of compounds in glucose uptake signaling pathways, immunoblot analysis was performed. As shown in Figure 4A, **2** dose dependently stimulated the phosphorylation of IRS-1 (Tyr⁹⁸⁹) and Akt (Ser⁴⁷³), which are key signaling molecules in insulin-mediated GLUT4 translocation. This was confirmed by the increase in the phosphorylation of GSK-3 β (Ser⁹) as a direct downstream target protein. Rosiglitazone (30 μM) and ursolic acid (10 μM) also increased the phosphorylation of both IRS-1 and Akt. The data in Figure 4B showed that **2** stimulated the phosphorylation of Erk1/2 (Thr²⁰²/Tyr²⁰⁴), but not AMPK (Thr¹⁷²) or the AMPK substrate ACC

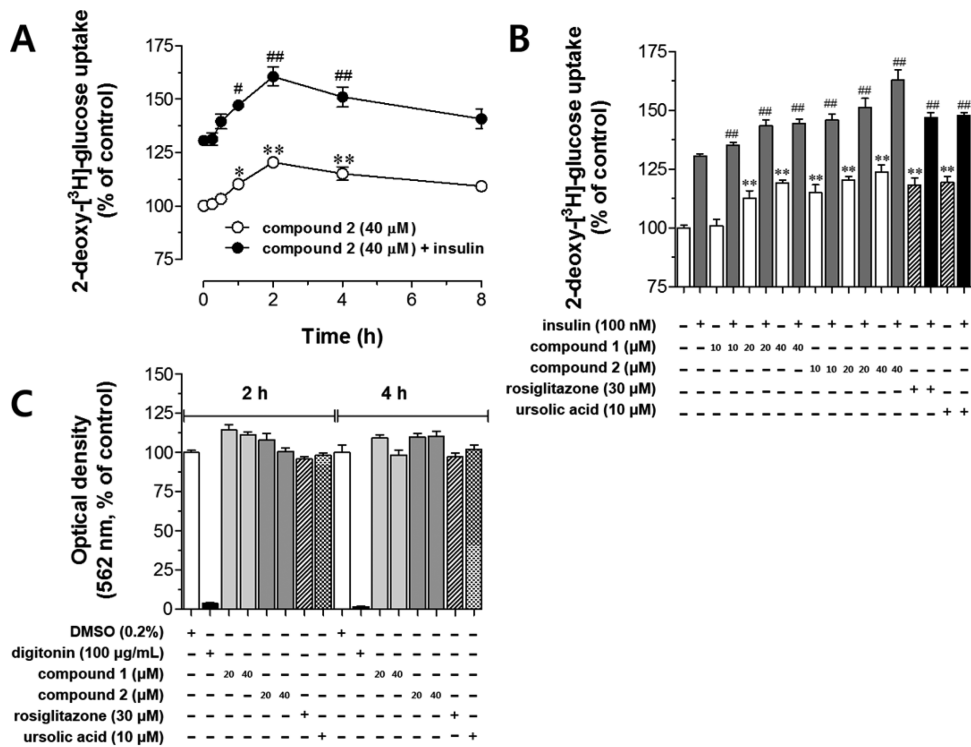


Figure 2. Compounds **1** and **2** enhance glucose uptake in C2C12 myotubes. (A) Time course of the effect of **2** on glucose uptake in C2C12 myotubes. Cells were treated with **2** (40 μM) alone or **2** (40 μM), followed by insulin (100 nM) for 30 min, and then incubated for the time periods indicated. Glucose uptake in the cell lysates was measured as described in the Experimental Section. (B) The dose–response relationship of the effects of **1** and **2** on glucose uptake in C2C12 myotubes. Cells were treated with **1** or **2** for 2 h. Rosiglitazone (30 μM) and ursolic acid (10 μM) were used as positive controls. (C) The cytotoxicities of **1** and **2** in C2C12 myotubes. C2C12 myotubes were treated with the indicated concentrations of compound for 2 or 4 h, and cell viability was examined at 562 nm by MTT assay. Digitonin (100 μg/mL) was used as the positive control. The results are expressed as means ± SEM of three independent experiments, each performed in triplicate. **p* < 0.05 and ***p* < 0.01, vs basal glucose uptake (no insulin stimulation); #*p* < 0.05 and ##*p* < 0.01, vs insulin-stimulated glucose uptake.

(Ser⁷⁹), in a dose-dependent manner. Taken together, **2** was found to significantly activate IRS-1, Akt, and Erk1/2 (Figure 4C). These results imply that, in addition to IRS-1 and Akt, Erk1/2 may, in part, play a role in **2**-mediated glucose uptake. Rosiglitazone, an activator of peroxisome proliferator-activated receptor γ (PPARγ) in adipose tissue and an AMPK activator in skeletal muscle,³⁹ significantly increased AMPK and slightly increased ACC phosphorylation in noninsulin treated groups. Similarly, **1** showed similar target protein activation as **2**. As shown in Figure 4D,E, IRS-1, Akt, GSK-3β, and Erk1/2 phosphorylation was stimulated by **1** in a dose-dependent manner (Figure 4F). Therefore, **1** and **2** activate the IRS-1-, Akt-, and Erk1/2-mediated signaling pathways; this activation was correlated with glucose uptake potency.

In the present study, rosiglitazone and ursolic acid were used as positive controls. Rosiglitazone increased the phosphorylation of AMPK under basal conditions but not significantly under insulin-stimulated conditions (Figure 4C). Regarding IRS-1/Akt, rosiglitazone stimulated the phosphorylation of these two signaling molecules only under insulin-stimulated conditions. Previous observations have shown that AMPK stimulation regulates IRS-1/Akt, and insulin and Akt have negative effects on AMPK activation.^{40,41} Moreover, in the skeletal muscle tissue of type 2 diabetic patients, rosiglitazone improves insulin receptor downstream signaling only under the insulin-stimulated state.⁴² Consistent with these observations, a decrease in AMPK activation by rosiglitazone under insulin-stimulated conditions may cause an increase in IRS-1/Akt activation. Ursolic acid, a pentacyclic triterpenoid, was reported to inhibit PTP-1B activity, leading

to stimulation of glucose uptake under basal and insulin-stimulated conditions.²¹ Moreover, ursolic acid enhances insulin receptor β subunit autophosphorylation and Akt and Erk1/2 phosphorylation.⁴³ The results shown in Figure 4C indicate that ursolic acid also stimulates the phosphorylation of IRS-1/Akt and Erk1/2 but not AMPK. However, the degree of Erk1/2 phosphorylation stimulated by **2** (40 μM) was greater than that by ursolic acid. These results suggest that the enhancement by **2** (with a C-27 carboxylic acid group) of glucose uptake was greater than that of ursolic acid (with a C-28 carboxylic acid group) (Figure 2B).

Because both **1** and **2** activate Akt, triciribine, an Akt selective inhibitor,⁴⁴ was used to investigate whether inhibition of Akt signaling blocked the ability of compounds to enhance glucose uptake. As shown in Figure 5A, **2** and 4 μM triciribine completely blocked the phosphorylation of Akt and GSK-3β, even following **2** treatment (40 μM); thus, 2 μM triciribine was selected for use in subsequent experiments. Under treatment with triciribine in C2C12 myotubes, the abilities of **1** and **2** to enhance glucose uptake were suppressed (Figure 5B,C). Both the basal and insulin-stimulated glucose uptake enhanced by 20 and 40 μM **2** was reduced significantly by triciribine treatment to 30.1% and 50.9% and 29.3% and 44.7%, respectively. Similarly, triciribine reduced both the basal and insulin-stimulated glucose uptake enhanced by 20 and 40 μM **1**. Data shown in Figure 5D indicate that GLUT4 translocation induced by **1** and **2** was reduced under Akt blockade in C2C12 myotubes. Thus, these results suggest that the Akt signaling pathway is critical for the increased glucose uptake induced by **1** and **2**.

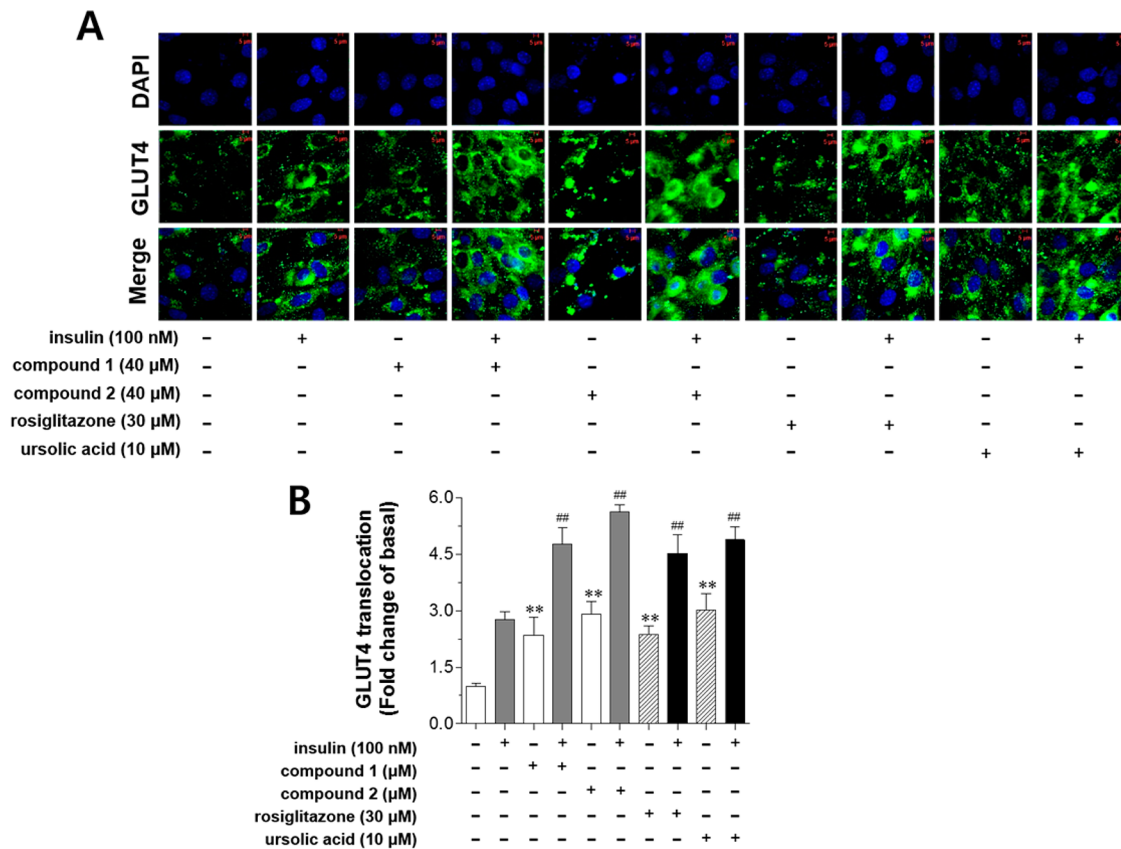


Figure 3. Enhancement of GLUT4 translocation from the cytoplasm to the plasma membrane by compounds **1** and **2**. (A) Confocal microscopy images of GLUT4 translocation in C2C12 myotubes. C2C12 myotubes were treated with 40 μ M of **1** or **2** alone for 2 h or **1** or **2** for 2 h followed by insulin (100 nM). Fluorescence intensities were measured using anti-GLUT4 and FITC-conjugated IgG. Scale bar = 5 μ m. (B) Quantification of confocal images. All values are means \pm SEM of three independent experiments. ** p < 0.01, vs the basal condition (no insulin stimulation); ## p < 0.01, vs the insulin-stimulated condition.

To determine the effect of Erk1/2 pathways on the stimulation of glucose uptake by **1** and **2**, C2C12 myotubes were pretreated with the MEK/ERK inhibitor U0126, and the effect of **1** and **2** on glucose uptake was measured. Data shown in Figure 6A illustrate that 10 and 20 μ M U0126 completely blocked Erk1/2 phosphorylation induced by 40 μ M **2**. Thus, 10 μ M U0126 was used for subsequent experiments. As expected, U0126 treatment reduced the abilities of **2** (Figure 6B) and **1** (Figure 6C) to enhance basal and insulin-stimulated glucose uptake. Interestingly, unlike triciribine, U0126 treatment had no significant effect on glucose uptake in the normal group (no insulin + no compound treatment) or insulin control group (insulin-treated, but no compound treatment). Moreover, in the compound-treated group, the decrease in glucose uptake rate mediated by U0126 was smaller than that of triciribine. The latter finding suggests that the Akt pathway is the main regulator of the enhancement of glucose uptake by **1** and **2**. Data shown in Figure 6D indicate that U0126 treatment suppressed the GLUT4 translocation stimulated by **1** and **2**. Thus, these results suggest that enhancement of glucose uptake by **1** and **2** is regulated, at least in part, by the Erk1/2 signaling pathway. In conclusion, this study has two new major findings: (1) compounds **1** and **2** enhance basal and insulin-stimulated glucose uptake in C2C12 myotubes, and (2) these compounds activate both the IRS-1/Akt and Erk1/2 pathways, subsequently inducing GLUT4 translocation. This is the first report that pentacyclic triterpenoids with a carboxylic acid group at C-27 isolated from *Astilbe rivularis* can enhance basal and insulin-stimulated glucose uptake. Thus, this unique scaffold may facilitate

development of novel agents for the management of blood glucose levels by improving insulin sensitivity and resistance.

EXPERIMENTAL SECTION

General Experimental Procedures. Optical rotation was measured by a JASCO P-2000 polarimeter (Tokyo, Japan). UV-vis spectra were measured using UV mini-1240 spectrophotometer (Shimadzu, USA). FT-IR data were recorded on Thermo Nicolet 380 (Madison, WI, USA). Nuclear magnetic resonance (NMR) experiments were conducted using a Bruker DMX 300 (1 H 300 MHz, 13 C 75 MHz), and Bruker DMX 600 (1 H 600 MHz, 13 C 150 MHz). Mass spectrometric data were obtained using a JMS 700 high-resolution mass spectrometer (JEOL, Japan). MPLC was carried out employing Biotage Isolera reversed-phase C₁₈ SNAP Cartridge KP-C₁₈-HS and normal-phase SNAP Cartridge KP-Sil (340 g; Biotage AB, Uppsala, Sweden). Thin-layer chromatography was performed on glass plates precoated with silica gel 60 F₂₅₄ and RP-18 F₂₅₄ (Merck, Darmstadt, Germany). Column chromatography was conducted in a silica gel column (70–230 mesh; Merck). For the glucose uptake inhibition bioassay, cell culture materials were purchased from Gibco BRL (Grand Island, NY, USA). 2-Deoxy-[3 H]-glucose was obtained from PerkinElmer Life Sciences (Boston, MA, USA). Rosiglitazone was purchased from Masung & Co., Ltd. (Seoul, Korea). Ursolic acid was available from our previous study. Antiphospho-IRS-1 (Tyr⁹⁸⁹) and anti-IRS-1 were from Santa Cruz Biotechnology (Santa Cruz, CA, USA). Antiphospho-Akt (Ser⁴⁷³), anti-Akt, antiphospho-glycogen synthase kinase 3 β (GSK-3 β) (Ser⁹), anti-GSK-3 β , anti-AMPK, antiphospho-acetyl-CoA carboxylase (ACC) (Ser⁷⁹), antiphospho-Erk1/2 (Thr²⁰²/Tyr²⁰⁴), and anti-Erk1/2 were from Cell Signaling Technology, Inc. (Beverly, MA, USA). Anti- β -actin and goat antirabbit antibodies were from Abfrontier (Geumcheon,

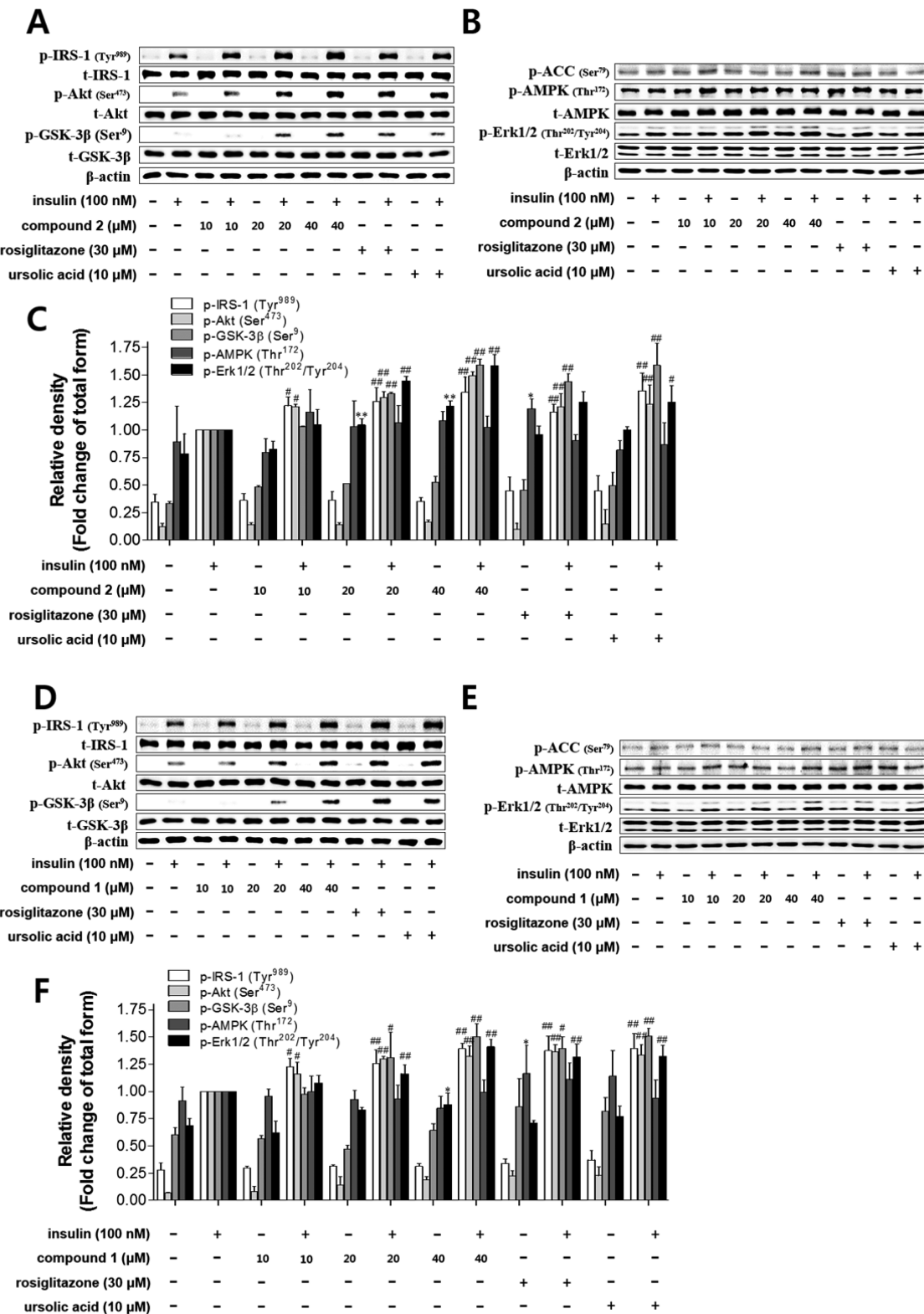


Figure 4. IRS-1, Akt, and Erk1/2 phosphorylation is enhanced by compounds **1** and **2** but not AMPK. After serum starvation for 2 h in DMEM, C2C12 myotubes were incubated with various concentrations of **1** or **2**, rosiglitazone (30 μ M), and ursolic acid (10 μ M) alone for 2 h, or **1** or **2**, rosiglitazone (30 μ M), and ursolic acid (10 μ M) for 2 h followed by insulin (100 nM) for 30 min. Cell lysates were resolved by SDS-PAGE, and immunoblotting was performed. (A,D) IRS-1, Akt, and GSK-3 β phosphorylation and (B,E) ACC, AMPK, and Erk1/2 phosphorylation. Gel images are representative of three independent experiments. (C,F) Relative density of protein phosphorylation. Values are means \pm SEM of three independent experiments. * $p < 0.05$ and ** $p < 0.01$ vs the basal condition (no insulin stimulation); # $p < 0.05$ and ## $p < 0.01$ vs the insulin-stimulated condition.

Seoul, Korea). Antiphospho-AMPK (Thr¹⁷²) was from Millipore Corporation (Billerica, MA, USA). Anti-GLUT4 was from Abcam

(Cambridge, MA, USA). Antifluorescein isothiocyanate (FITC) was from Sigma (St. Louis, MO, USA). Triciribine and U0126 were from

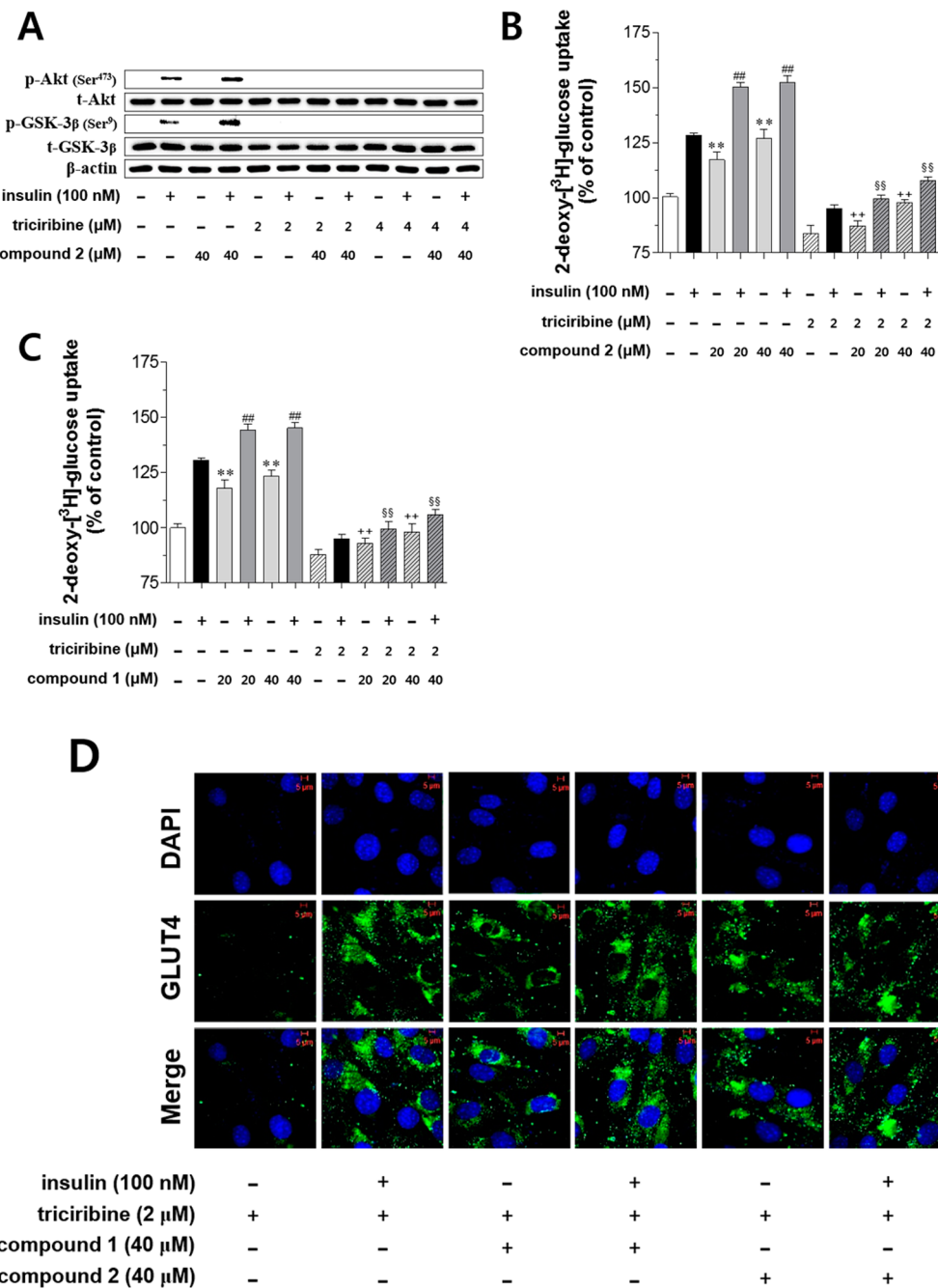


Figure 5. Involvement of the Akt-mediated pathway in compounds 1- and 2-induced stimulation of glucose uptake. (A) Inhibition of the Akt-mediated pathway by the Akt inhibitor triciribine. C2C12 myotubes were pretreated with the indicated concentrations of triciribine for 30 min and incubated with 40 μ M 2 alone for 2 h, or 40 μ M 2 followed by insulin (100 nM). Cell lysates were resolved by SDS-PAGE, and immunoblotting was performed. Gel images are representative of three experiments. (B,C) Effect of 1 and 2 on glucose uptake in triciribine-pretreated C2C12 myotubes. C2C12 myotubes were pretreated with 2 μ M triciribine for 30 min and incubated with 1 or 2 alone for 2 h, or 1 or 2 for 2 h followed by 100 nM insulin. Glucose uptake was measured as described in the Experimental Section. Values are means \pm SEM of three independent experiments. **p < 0.01 vs basal glucose uptake (no insulin stimulation); ##p < 0.01 vs insulin-stimulated glucose uptake; ++p < 0.01 vs compound-treated basal glucose uptake; §§p < 0.01 vs compound-treated insulin-stimulated glucose uptake. (D) Confocal microscopy images of GLUT4 translocation in C2C12 myotubes. C2C12 myotubes pretreated with 2 μ M triciribine were incubated with 40 μ M of 1 or 2 alone for 2 h, or 1 or 2 for 2 h followed by 100 nM insulin. Fluorescence intensities were measured using anti-GLUT4 and FITC-conjugated IgG as described in the Experimental Section. Scale bar = 5 μ m.

Enzo (Enzo Life Sciences AG, Lausen, Switzerland). Other chemicals were of analytical grade.

Plant Material. The roots of *A. rivularis* were collected from Sapa, Vietnam in September 2011, and were identified by Dr. Phuong Thien Thuong (National Institute of Medicinal Materials, Vietnam) and Professor MinKyun Na (College of Pharmacy, Chungnam National University, Korea). A voucher specimen was deposited at the herbaria of

the Vietnam National Institute of Medicinal Materials (VDL-01/2011–01), Hanoi, Vietnam, and the Laboratory of Pharmacognosy at the College of Pharmacy (CNU 00196), Chungnam National University, Daejeon, Korea.

Extraction and Isolation. Dried roots of *A. rivularis* (3 kg) were extracted twice with methanol (10 L \times 2) at room temperature for 1 week and filtered. The methanol extract (200 g) was suspended in H₂O (2 L) and partitioned with *n*-hexane (2 L \times 3), ethyl acetate (2 L \times 3),

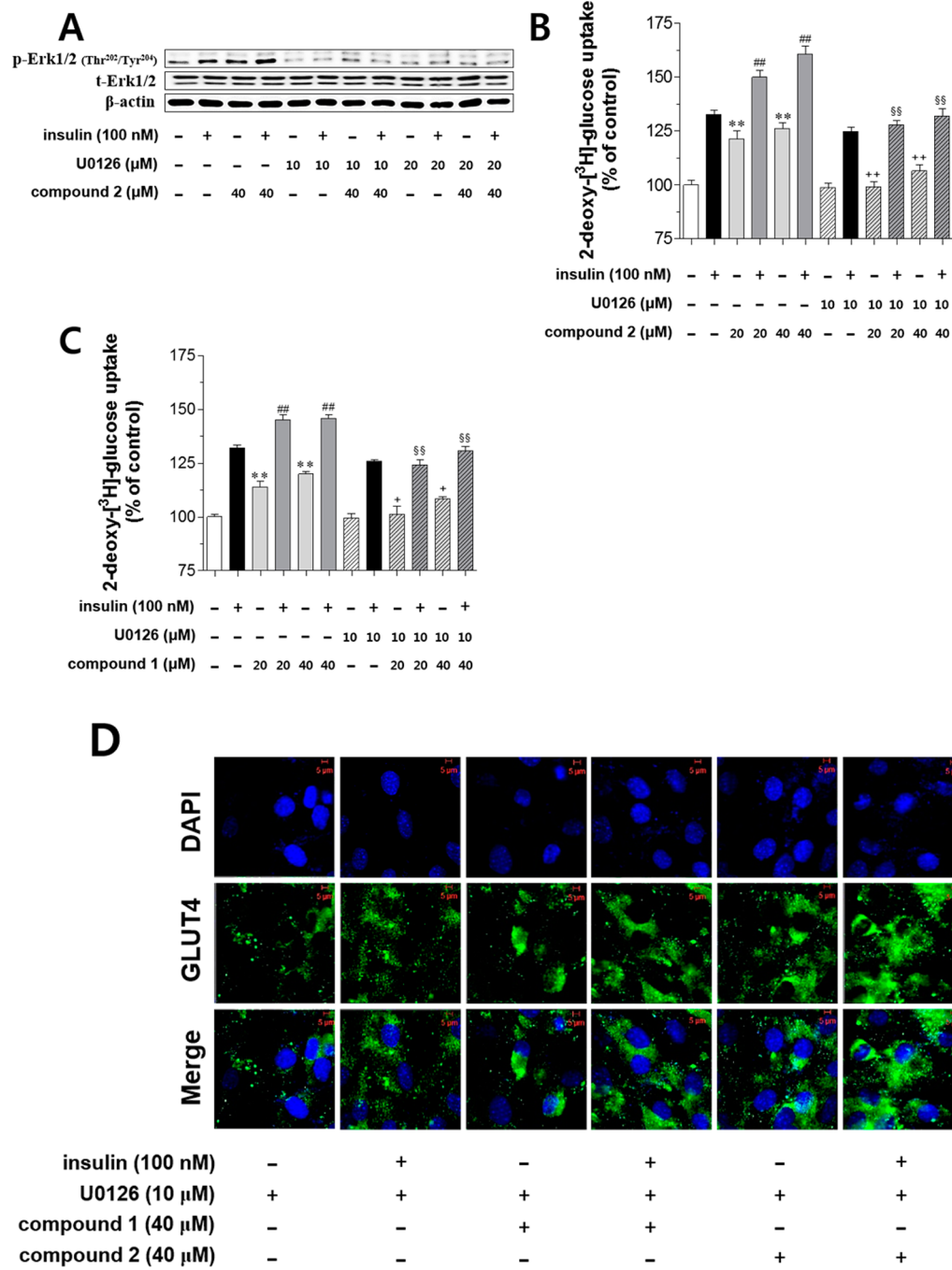


Figure 6. Involvement of the Erk1/2-mediated pathway in compound-induced stimulation of glucose uptake. (A) Inhibition of the Erk1/2-mediated pathway by the MEK/ERK inhibitor U0126. C2C12 myotubes were pretreated with the indicated concentrations of U0126 for 30 min, and then with 40 μ M 2 alone for 2 h, or 40 μ M 2 for 2 h followed by insulin (100 nM). Cell lysates were resolved by SDS-PAGE, and immunoblotting was performed. Gel images are representative of three experiments. (B,C) Effects of 1 and 2 on glucose uptake in U0126-pretreated C2C12 myotubes. C2C12 myotubes pretreated with 10 μ M U0126 for 30 min were incubated with either 1 or 2 alone for 2 h or 1 or 2 for 2 h followed by 100 nM insulin. Glucose uptake was then measured. Values are means \pm SEM of three independent experiments. ** p < 0.01, vs basal glucose uptake (no insulin stimulation); ## p < 0.01 vs insulin-stimulated glucose uptake; + p < 0.05 and ++ p < 0.01 vs compound-treated basal glucose uptake; §§ p < 0.01 vs compound-treated insulin-stimulated glucose uptake. (D) Confocal microscopy images of GLUT4 translocation in C2C12 myotubes. C2C12 myotubes pretreated with 10 μ M U0126 were incubated with either 40 μ M 1 or 2 alone for 2 h or 40 μ M 1 or 2 for 2 h followed by 100 nM insulin. Fluorescence intensities were measured using anti-GLUT4 and FITC-conjugated IgG. Scale bar = 5 μ m.

and *n*-butanol (2 L \times 3) to yield *n*-hexane-, ethyl acetate-, *n*-butanol- (55, 27, 50 g, respectively), and H₂O-soluble fraction. The *n*-hexane fraction (55 g) was subjected to silica gel medium-pressure liquid chromatography (MPLC) (SNAP Cartridge KP-Sil, 340 g) with a gradient of *n*-hexane–ethyl acetate (95:5 \rightarrow 50:50) to give 10 fractions (Fr. H1–H10). Fr. H4 (3 g) was further fractionated into nine

subfractions (Fr. H41–H49) utilizing MPLC (C₁₈ SNAP cartridge KP-C₁₈–HS, 120 g) eluting with methanol–H₂O (78:22 \rightarrow 96:4). Fr. H44 (230 mg) was chromatographed over a silica gel column (2 cm \times 80 cm) and eluted with *n*-hexane–ethyl acetate–acetone (5:1:0.15) to obtain 2 (8 mg). Compound 1 (50 mg) was obtained from Fr. H49 (312 mg) using a silica gel column (2 \times 80 cm) with an *n*-hexane–ethyl acetate–acetone

(7:1:0.1) elution solvent. Fr. HS (3.3 g) was separated using reversed-phase MPLC (C_{18} SNAP cartridge KP- C_{18} -HS, 120 g) eluted with methanol-H₂O (75:25 → 95:5) to yield seven subfractions (Fr. H51–H57). Fr. HS6 (450 mg) was subjected to silica gel column (2.5 cm × 80 cm) chromatography with *n*-hexane–ethyl acetate–acetone (6.5:1:0.1, 5.2:1:0.1, 800 mL for each step) to obtain 3 β -hydroxyolean-12-en-27-oic acid³⁰ (200 mg) and 3 β ,6 β ,7 α -trihydroxyolean-12-en-27-oic acid³² (8.5 mg). Fr. H8 (1.3 g) was purified by MPLC (C_{18} SNAP cartridge KP- C_{18} -HS, 120 g) eluted with methanol-H₂O (77:23 → 92:8) to produce five subfractions (Fr. H81–H85). Fr. H83 (33 mg) was separated using a silica gel column (1.5 cm × 80 cm) with an *n*-hexane–ethyl acetate (2.5:1) elution solvent to produce 3 β ,6 β -dihydroxyolean-12-en-27-oic acid³⁰ (13 mg). 3 β ,24-Dihydroxyolean-12-en-27-oic acid³¹ (23.6 mg) was purified from Fr. H84 (275 mg) using a silica gel column (2 cm × 80 cm) eluted with *n*-hexane–ethyl acetate–methanol (3.5:1:0.1). The purities of compounds **1** (98.7%) and **2** (99.1%) were determined by HPLC with an evaporative light scattering detector (Figure S16, Supporting Information).

3 β -trans-p-Coumaroyloxy-olean-12-en-27-oic acid (1): White amorphous powder; $[\alpha]_D^{20} +25.1$ (*c* 0.1, CHCl₃); UV (CHCl₃) λ_{max} (log ϵ) 293 (4.37), 306 (4.35) nm; IR (KBr) ν_{max} 3310, 2948, 1683, 1586 cm⁻¹; ¹H and ¹³C NMR, see Table 1; HRESIMS *m/z* 625.3870 [M + Na]⁺ (calcd for C₃₉H₅₄O₅Na, 625.3869).

Cell Culture and Differentiation. Mouse muscle myoblasts C2C12 were grown in Dulbecco's Modified Eagle's Medium (DMEM) with 10% fetal bovine serum (FBS) at 37 °C in a 5% CO₂ atmosphere. Confluent myoblasts were differentiated by incubation in DMEM containing 1% FBS. The medium was replaced every day until day 4.^{45,46} Compounds were dissolved in dimethyl sulfoxide (DMSO), the final concentration of which in the medium was not greater than 0.3%.

Cell Viability Assay. Cell viability was examined using a 3-(4,5-dimethylthiazol-2-yl)-2,5-diphenyltetrazolium bromide (MTT) assay. Differentiated C2C12 myotubes in 96-well culture plates were treated with various concentrations of the test compounds or 100 μ g/mL digitonin as a cytotoxic control. Cells were incubated for a given time, and MTT reagent (5 mg/mL) was added to each well. After 2 h, cells were treated with 200 μ L of DMSO, and the absorbance at 565 nm was measured using a microplate reader (Tecan Group Ltd., Männedorf, Switzerland).

Glucose Uptake Assay. The glucose uptake assay was performed as described previously with minor modifications.⁴⁷ C2C12 myotubes seeded in a 24-well microplate were serum-starved in DMEM with 0.2% bovine serum albumin (BSA), and the cells were incubated in Krebs–Ringer phosphate-HEPES (KRPH) buffer (10 mM HEPES, pH 7.4, 136 mM NaCl, 4.7 mM KCl, 1 mM MgSO₄, 1 mM CaCl₂, 10 mM phosphate buffer). Compounds were treated with medium alone or followed by 100 nM insulin for 30 min. Glucose uptake was initiated by the addition of 0.5 μ Ci/mL 2-deoxy-[³H]-glucose with 100 μ M 2-deoxy-D-glucose to each well. After 10 min, cells were washed three times with ice-cold phosphate-buffered saline (PBS, pH 7.4) and lysed with 0.1% sodium dodecyl sulfate (SDS) and 0.5 M NaOH. The radioactivity was determined using liquid scintillation counting in a β -counter and normalized according to the total protein level.

Immunoblot Analysis. After treatment, C2C12 myotubes were washed twice in ice-cold PBS and lysed using ice-cold RIPA buffer (50 mM Tris-HCl, pH 8.0, 150 mM NaCl, 1.0% NP-40, 2 mM EDTA, 5 mM NaF, 1 mM PMSF, 1 mM sodium orthovanadate, 0.5% sodium deoxycholate, and 0.1% sodium dodecyl sulfate). Lysates were incubated at 4 °C for 30 min and then centrifuged at 8000g for 10 min at 4 °C to remove insoluble materials. The protein concentrations were determined using a BCA protein assay kit (Pierce, Rockford, IL, USA). For each blot, equal amounts of cell lysates (10–20 μ g of protein) were separated by SDS-polyacrylamide gel electrophoresis (SDS-PAGE, 7.5–12.5%) and transferred onto polyvinylidene fluoride (PVDF) membranes (ATTO Corp., Tokyo, Japan) at 200 mA for 2 h. The blots were blocked with 5% BSA in TBS-T (20 mM Tris-Base, 137 mM NaCl at pH 7.4 and 0.05% Tween-20) at 4 °C for 1.5 h and incubated with appropriate primary antibodies at 4 °C overnight and subsequently with a secondary antibody. Protein bands were detected using the ECL kit

(ATTO Corp., Tokyo, Japan), and the intensities of bands were quantified using the Image Lab software (Bio-Rad, Hercules, CA, USA).

Detection of Cell Surface GLUT4 by Immunofluorescence.

Immunofluorescence was performed using a method published previously, with slight modifications.⁴⁸ Following treatment of C2C12 myotubes differentiated on glass coverslips, cells were washed twice with PBS and fixed with 4% formaldehyde in PBS for 15 min and quenched with 100 mM glycine in PBS for 10 min. Cells were blocked with 5% goat serum in PBS for 1 h and incubated with anti-GLUT4 antibody (1:200 dilution in 3% BSA in PBS) for 1.5 h. After washing with PBS, cells were incubated with secondary antibody (FITC-IgG; 1:200 dilution in 3% BSA in PBS) for 1.5 h. Cells were washed with PBS and mounted with Mounting Medium with 6,4'-diamidino-2-phenylindole (DAPI) (Vector Laboratories Inc., Burlingame, CA, USA). Images were obtained using a confocal laser microscope (LSMS live configuration Variotwo VRGB; Zeiss, Jena, Germany). Quantification of immunocytochemistry images was performed using the ImageJ software (NIH).

Statistical Analysis. All values are expressed as means ± standard error of the mean (SEM). Statistical comparisons of the results were tested using Dunnett's multiple comparison test using the GraphPad Prism software (San Diego, CA, USA). A *p* value less than 0.05 was deemed to indicate statistical significance.

ASSOCIATED CONTENT

S Supporting Information

NMR spectra, HRESIMS data, and IR spectra of compounds **1** and **2**. This material is available free of charge via the Internet at <http://pubs.acs.org>.

AUTHOR INFORMATION

Corresponding Authors

*For C.S.M.: Phone: +82 42 821 5923. Fax: +82 42 821 8925. E-mail: cm8r@cnu.ac.kr.

*For M.N.: Phone: +82 42 821 5925. Fax: +82 42 823 6566. E-mail: mkna@cnu.ac.kr.

Author Contributions

▀ J. H. Han and W. Zhou contributed equally.

Notes

The authors declare no competing financial interest.

ACKNOWLEDGMENTS

This work was supported by the National Research Foundation of Korea (NRF) grant (nos. 2010-0014839 and 2014R1A2A2A01006793) and the Priority Research Centers Program (no. 2009-0093815), funded by the Ministry of Education, Science, and Technology (MEST).

REFERENCES

- Parker, J. C. *Adv. Drug Delivery Rev.* **2002**, *S4*, 1173–1197.
- Zhou, Q. G.; Hou, F. F.; Guo, Z. J.; Liang, M.; Wang, G. B.; Zhang, X. *Diabetes Metab. Res. Rev.* **2008**, *24*, 459–464.
- Kumar, N.; Dey, C. S. *Br. J. Pharmacol.* **2002**, *137*, 329–336.
- Huang, S.; Czech, M. P. *Cell Metab.* **2007**, *5*, 237–252.
- Bryant, N. J.; Govers, R.; James, D. E. *Nature Rev. Mol. Cell Biol.* **2002**, *3*, 267–277.
- Huang, C.; Thirone, A. C.; Huang, X.; Klip, A. *J. Biol. Chem.* **2005**, *280*, 19426–19435.
- White, M. F. *Am. J. Physiol. Endocrinol. Metab.* **2002**, *283*, E413–422.
- Bouzakri, K.; Zachrisson, A.; Al-Khalili, L.; Zhang, B. B.; Koistinen, H. A.; Krook, A.; Zierath, J. R. *Cell Metab.* **2006**, *4*, 89–96.
- Pu, J.; Peng, G.; Li, L.; Na, H.; Liu, Y.; Liu, P. *J. Lipid Res.* **2011**, *52*, 1319–1327.
- Chen, S.; Mackintosh, C. *Cell. Signalling* **2009**, *21*, 1984–1993.
- Gual, P.; Le Marchand-Brustel, Y.; Tanti, J. *Diabetes Metab.* **2003**, *29*, 566–575.

- (12) Lin, W.; Huang, X.; Zhang, L.; Chen, D.; Wang, D.; Peng, Q.; Xu, L.; Li, J.; Liu, X.; Li, K.; Ding, K.; Jin, S.; Li, J.; Wu, D. *PLoS One* **2012**, *7*, e44570.
- (13) Geiger, P. C.; Wright, D. C.; Han, D. H.; Holloszy, J. O. *Am. J. Physiol. Endocrinol. Metab.* **2005**, *288*, E782–788.
- (14) Turban, S.; Beardmore, V. A.; Carr, J. M.; Sakamoto, K.; Hajduch, E.; Arthur, J. S.; Hundal, H. S. *Diabetes* **2005**, *54*, 3161–3168.
- (15) Bettaiel, A.; Matsuo, K.; Matsuo, I.; Wang, S.; Melhem, R.; Koromilas, A. E.; Haj, F. G. *PLoS One* **2012**, *7*, e34412.
- (16) Koren, S.; Fantus, I. G. *Best Pract. Res. Clin. Endocrinol. Metab.* **2007**, *21*, 621–640.
- (17) Bakhtiyari, S.; Meshkani, R.; Taghikhani, M.; Larijani, B.; Adeli, K. *Lipids* **2010**, *45*, 237–244.
- (18) Tsuchiya, A.; Kanno, T.; Nishizaki, T. *Cell. Physiol. Biochem.* **2013**, *32*, 1451–1459.
- (19) Pitschmann, A.; Zehl, M.; Atanasov, A. G.; Dirsich, V. M.; Heiss, E.; Glasl, S. J. *Ethnopharmacol.* **2014**, *152*, 599–602.
- (20) Na, M.; Cui, L.; Min, B. S.; Bae, K.; Yoo, J. K.; Kim, B. Y.; Oh, W. K.; Ahn, J. S. *Bioorg. Med. Chem. Lett.* **2006**, *16*, 3273–3276.
- (21) Zhang, W.; Hong, D.; Zhou, Y.; Zhang, Y.; Shen, Q.; Li, J. Y.; Hu, L. H.; Li, J. *Biochim. Biophys. Acta* **2006**, *1760*, 1505–1512.
- (22) Shi, L.; Zhang, W.; Zhou, Y. Y.; Zhang, Y. N.; Li, J. Y.; Hu, L. H.; Li, J. *Eur. J. Pharmacol.* **2008**, *584*, 21–29.
- (23) Tan, M. J.; Ye, J. M.; Turner, N.; Hohnen-Behrens, C.; Ke, C. Q.; Tang, C. P.; Chen, T.; Weiss, H. C.; Gesing, E. R.; Rowland, A.; James, D. E.; Ye, Y. *Chem. Biol.* **2008**, *15*, 263–273.
- (24) Ha do, T.; Tuan, D. T.; Thu, N. B.; Nhieu, N. X.; Ngoc, T. M.; Yim, N.; Bae, K. *Bioorg. Med. Chem. Lett.* **2009**, *19*, 5556–5559.
- (25) Paiva dos Santos, R.; L, T. L. G.; Pessoa, O. D. L.; Braz-Filho, R.; Rodrigues-Filho, E.; Viana, F. A.; Silveira, E. R. *J. Brazil. Chem. Soc.* **2005**, *16*, 662–665.
- (26) Efidi, M.; Ninomiya, M.; Suryani, E.; Tanaka, K.; Ibrahim, S.; Watanabe, K.; Koketsu, M. *Bioorg. Med. Chem. Lett.* **2012**, *22*, 4242–4245.
- (27) Verma, V. K.; S, N. U.; Aslam, M. *Int. J. Pharm. Sci. Rev. Res.* **2011**, *7*, 93–95.
- (28) Lu, M. Y.; Liao, Z. X.; Ji, L. J.; Sun, H. F. *Fitoterapia* **2013**, *85*, 119–124.
- (29) Van le, T. K.; Hung, T. M.; Thuong, P. T.; Ngoc, T. M.; Kim, J. C.; Jang, H. S.; Cai, X. F.; Oh, S. R.; Min, B. S.; Woo, M. H.; Choi, J. S.; Lee, H. K.; Bea, K. *J. Nat. Prod.* **2009**, *72*, 1419–1423.
- (30) Sun, H. X.; Z, J. X.; Ye, Y. P.; Pan, Y. J.; Shen, Y. A. *Helv. Chim. Acta* **2003**, *86*, 2414–2423.
- (31) Cai, X. F.; Park, B. Y.; Ahn, K. S.; Kwon, O. K.; Lee, H. K.; Oh, S. *R. J. Nat. Prod.* **2009**, *72*, 1241–1244.
- (32) Hu, J. Y.; Yao, Z.; Xu, Y. Q.; Takaishi, Y.; Duan, H. Q. *J. Asian Nat. Prod. Res.* **2009**, *11*, 236–242.
- (33) Zhang, W. Y.; Lee, J. J.; Kim, I. S.; Kim, Y.; Myung, C. S. *Pharmacology* **2011**, *88*, 266–274.
- (34) Heiss, E. H.; Baumgartner, L.; Schwaiger, S.; Heredia, R. J.; Atanasov, A. G.; Rollinger, J. M.; Stuppner, H.; Dirsich, V. M. *Planta Med.* **2012**, *78*, 678–681.
- (35) Eid, S. Y.; El-Readi, M. Z.; Wink, M. *Phytomedicine* **2012**, *19*, 1307–1314.
- (36) Rowland, A. F.; Fazakerley, D. J.; James, D. E. *Traffic* **2011**, *12*, 672–681.
- (37) Taniguchi, C. M.; Emanuelli, B.; Kahn, C. R. *Nature Rev. Mol. Cell Biol.* **2006**, *7*, 85–96.
- (38) Previs, S. F.; Withers, D. J.; Ren, J. M.; White, M. F.; Shulman, G. I. *J. Biol. Chem.* **2000**, *275*, 38990–38994.
- (39) Fryer, L. G.; Parbu-Patel, A.; Carling, D. *J. Biol. Chem.* **2002**, *277*, 25226–25232.
- (40) Tao, R.; Gong, J.; Luo, X.; Zang, M.; Guo, W.; Wen, R.; Luo, Z. J. *Mol. Signaling* **2010**, *5*, 1.
- (41) Zou, F.; Mao, X. Q.; Wang, N.; Liu, J.; Ou-Yang, J. P. *Acta Pharmacol. Sin.* **2009**, *30*, 1607–1615.
- (42) Miyazaki, Y.; He, H.; Mandarino, L. J.; DeFronzo, R. A. *Diabetes* **2003**, *52*, 1943–1950.
- (43) Jung, S. H.; Ha, Y. J.; Shim, E. K.; Choi, S. Y.; Jin, J. L.; Yun-Choi, H. S.; Lee, J. R. *Biochem. J.* **2007**, *403*, 243–250.
- (44) Yang, L.; Dan, H. C.; Sun, M.; Liu, Q.; Sun, X. M.; Feldman, R. I.; Hamilton, A. D.; Polokoff, M.; Nicosia, S. V.; Herlyn, M.; Sebti, S. M.; Cheng, J. Q. *Cancer Res.* **2004**, *64*, 4394–4399.
- (45) Park, C. E.; Kim, M. J.; Lee, J. H.; Min, B. I.; Bae, H.; Choe, W.; Kim, S. S.; Ha, J. *Exp. Mol. Med.* **2007**, *39*, 222–229.
- (46) Han, J. H.; Kim, I. S.; Jung, S. H.; Lee, S. G.; Son, H. Y.; Myung, C. S. *PLoS One* **2014**, *9*, e95268.
- (47) Kim, K. Y.; Cho, H. S.; Jung, W. H.; Kim, S. S.; Cheon, H. G. *Mol. Pharmacol.* **2007**, *71*, 1554–1562.
- (48) Bisht, B.; Dey, C. S. *BMC Cell Biol.* **2008**, *9*, 48.